

The Role of Coastal Upwelling in Suppressing the Warming Trend of Sea Surface Temperature along the Southern Coast of Java

Daenk Himawa¹, Anindya Wirasatriya^{1*}, Kunarso¹, Parichat Wetchayont²

¹Department of Oceanography, Faculty of Fisheries and Marine Science, Diponegoro University
Jl. Prof. Jacub Rais Tembalang Semarang Jawa Tengah 50275, Indonesia

²Disaster Management Program, Faculty of Science and Health Technology, Navamindradhiraj University
Bangkok 10300, Thailand

Email: anindyawirasatriya@lecturer.undip.ac.id

Abstract

This study examines the unclear role of wind-driven upwelling through Ekman transport and pumping, along with the combined effects of the Indian Ocean Dipole (IOD) and El Niño-Southern Oscillation (ENSO) trends on the warming rate of Sea Surface Temperature (SST) along the southern coast of Java. Using data from 1940 to 2023, we investigated how IOD, ENSO, Ekman transport, and Ekman pumping influence SST trends. Our results reveal a cooling trend in SST near the coast during the upwelling period and a warming trend across the entire area during the non-upwelling period. The cooling SST weakens the easterly winds passing through the coastal areas, reducing upwelling intensity, as indicated by the weakening of Ekman transport. However, Ekman pumping, another proxy for upwelling, shows a strengthening trend. Our comparison along coastal areas suggests that the increase in Ekman pumping is more robust than the decrease in Ekman transport, leading to an overall intensification of upwelling. Additionally, we observed positive trends in IOD and ENSO during the upwelling period. These trends significantly enhance the upwelling process and are responsible for the observed cooling trend in SST. Thus, while wind-driven upwelling through Ekman transport and pumping plays a crucial role as a key process, its intensification is primarily driven by the trends in IOD and ENSO.

Keywords: global warming, coastal upwelling, SST, IOD, ENSO

Introduction

Coastal upwelling is when cold, nutrient-rich water from deeper ocean layers rises to the surface due to wind-driven offshore transport. This results in a cooling effect on coastal surface waters, counteracting the typically warm surface temperatures in ocean regions. As global warming progresses and SST increases, distinct variations in the warming rates of SST are observed between coastal and oceanic areas. These variations are particularly evident in regions experiencing upwelling, such as Canary (Santos *et al.*, 2012a), Benguela (Santos *et al.*, 2012b), La Guajira (Santos *et al.*, 2016), and the Yucatan Peninsula (Varela *et al.*, 2018a).

The process of upwelling, which regulates the warming trend of SST, is experiencing changes in intensity as well. Global warming, as hypothesized by Bakun (1990), induces variations in land-sea heating, amplifying the air pressure gradient, and thereby strengthening alongshore winds that intensify coastal upwelling. However, the impact of global warming on coastal upwelling yields varied outcomes. Major upwelling systems such as the Benguela, California, Humboldt, and Canary-Iberian are intensifying, as

Satar *et al.* (2023) detailed. Nevertheless, the effect on local seasonal upwelling remains uncertain. Upwelling in some marginal seas, such as the Taiwan Strait (Zhang, 2021), the Banda Sea (Rachman *et al.*, 2020), and the Alboran Sea (Mercado *et al.*, 2012), exhibits a decrease in wind-driven upwelling, contrary to Bakun's hypothesis, while others, like La Guajira (Santos *et al.*, 2016), show an increase. According to Varela *et al.* (2015), the effects of changing upwelling intensity vary depending on location, study duration, season, and data sources. Therefore, further research is essential to fully grasp the long-term changes in the upwelling system's projection.

Varela *et al.* (2016) investigated the differences in SST warming trends between coastal and oceanic areas and the trend in upwelling intensity along the southern coast of Java. They analyzed sea temperature trends across vertical layers, the Upwelling Index (UI) based on Ekman transport, and heat flux. Their findings suggest the observed cooling SST trend in coastal areas is not linked to the UI trend, which shows a weakening pattern. Instead, the cooling trend is associated with changes in the vertical structure of the water column. However, their study did not address several factors influencing upwelling and SST trends, such as IOD (Horie *et al.*,

2018) and ENSO (Susanto *et al.*, 2001), which have proven to affect the strength of upwelling along the southern coast of Java. Moreover, in the same area, Wirasatriya *et al.* (2020) found that Ekman transport alone is insufficient to explain the distinct spatial patterns of wind-driven upwelling and its relationship to SST. Their findings underscore the necessity of considering Ekman pumping, which represents vertical water movement, to explain the spatial distribution of wind-driven upwelling and its correlation with SST.

In light of previous research, it is essential to re-examine the trends in wind-driven upwelling intensity by incorporating both Ekman transport and pumping. Additionally, since climate events such as IOD and ENSO significantly impact SST, their trends must also be considered. This study aims to address a gap in the existing literature by analyzing data from 1940 to 2023 to provide insights into the relationship between the trends of upwelling, climate events, and their effects on SST under global warming conditions, especially along the southern coast of Java. In this region, upwelling is crucial for supporting the fisheries industry. For instance, during the upwelling period, bigeye tuna catches significantly increased, especially during positive phases of IOD or *El Niño* events, as observed by Lumban-Gaol *et al.* (2015). Similarly, Koropitan *et al.* (2021) noted increased mackerel tuna catches during these events, reinforcing the patterns observed for bigeye tuna. Moreover, Wen *et al.* (2023) highlighted that the impact of upwelling influenced by climate events extends beyond catch quantities to affect the distribution of commercial fish stocks along the southern coast of Java. Therefore, a more detailed examination of upwelling changes is necessary to improve predictions and readiness for the fisheries industry.

Materials and Methods

Long-term data is essential for studying trends related to global warming, as it enables the detection of subtle changes over an extended period. Therefore, data from the European Centre for Medium-Range Weather Forecasts ReAnalysis 5 (ERA5) were utilized due to its extensive historical coverage. Monthly sea surface winds at 10 meters above sea level and SST for the period 1940–2023 were downloaded from the Climate Data Store website (<https://cds.climate.copernicus.eu/>). Both wind and SST data have a consistent spatial resolution of $0.25^\circ \times 0.25^\circ$.

It is essential to compare ERA5, which combines model and observational data globally, with remote sensing data to validate the accuracy and reliability of the information. Advanced Scatterometer

(ASCAT) and Operational Sea Surface Temperature and Ice Analysis (OSTIA) were employed as reference datasets. For more detailed information on these datasets, please refer to Remmers *et al.* (2019) for ASCAT and Donlon *et al.* (2012) for OSTIA. The validation results, depicted in Figure 1, reveal a consistent pattern and a low Root Mean Square Error (RMSE) value of less than 0.5 for both wind components and SST datasets, signifying a robust agreement among ASCAT, OSTIA, and ERA5 data.

Moreover, it is vital to consider IOD and ENSO, as they are pivotal interannual events that greatly influence upwelling on the southern coast of Java. Researchers track these phenomena using the Dipole Mode Index (DMI) and the *Niño* 3.4 index, which are standard indicators for identifying and observing IOD and ENSO events (Saji *et al.*, 1999; Bunge and Clarke, 2009). The relevant data can be accessed through the National Oceanic and Atmospheric Administration (NOAA) website (<https://psl.noaa.gov/gcoswgs/TimeSeries/>).

After verifying the reliability of the data, Ekman transport and pumping were calculated to represent the upwelling phenomenon, following the methodologies applied by Varela *et al.* (2016) and Wirasatriya *et al.* (2020). However, unlike Varela *et al.* (2016), the UI was not computed based on Ekman transport due to the east-west horizontal elongation of Java Island, as illustrated in Figure 2. This geographical feature allows the offshore-onshore water movement to be effectively represented by the meridional component of Ekman transport, following the approach by Wirasatriya *et al.* (2020). The equations are as follows:

$$W = (W_x^2 + W_y^2)^{1/2}$$

$$\tau_x = \rho_a C_d W W_x \text{ and } \tau_y = \rho_a C_d W W_y$$

$$M_x = \frac{\tau_y}{\rho_w f} \text{ and } M_y = -\frac{\tau_x}{\rho_w f}$$

Where W is the wind speed ($m s^{-1}$), calculated by the monthly zonal (W_x) and meridional (W_y) wind components. τ is the wind stress ($N m^{-3}$), calculated by the air density ($\rho_a = 1.25 kg m^{-3}$), the wind components, and the drag coefficient (C_d) which followed (Wamdi, 1988):

$$\text{for } 0 m s^{-1} < W \leq 7.5 m s^{-1}, \text{ then } C_d = 1.29 \times 10^{-3}$$

$$\text{for } 7.5 m s^{-1} < W \leq 50 m s^{-1}, \text{ then } C_d = (0.8 + 0.0065W) \times 10^{-3}$$

M_x and M_y are the zonal and meridional Ekman transport ($m^2 s^{-1}$), calculated by the wind stress, the water density ($\rho_w = 1025 kg m^{-3}$), and the Coriolis force (f), which calculated from $f = 2\Omega \sin \varphi$, where $\Omega = 7.292 \times 10^{-3}$ is the speed of the Earth's

rotation, which value refers to Stewart (2008) and φ is the latitude.

$$\nabla \times \tau = \frac{\partial \tau_y}{\partial x} - \frac{\partial \tau_x}{\partial y}$$

$$w = \frac{\nabla \times \tau}{\rho_w f}$$

Ekman pumping (w ; in unit of m s^{-1}) is calculated by the wind-stress curl ($\nabla \times \tau$), the water density, and the Coriolis force.

Before calculating the trend, the monthly data were converted to annual averages. For both wind and SST, averages were computed for the periods of December to February and July to September, representing the northwest and southeast monsoons, respectively (Susanto *et al.*, 2001; Wirasatriya *et al.*, 2020, 2021). This approach facilitated a comparison of trends between non-upwelling and upwelling periods. Linear regression analysis was then applied to determine the trend, with the slope value calculated per decade. To facilitate interpretation, the meridional Ekman transport and Ekman pumping

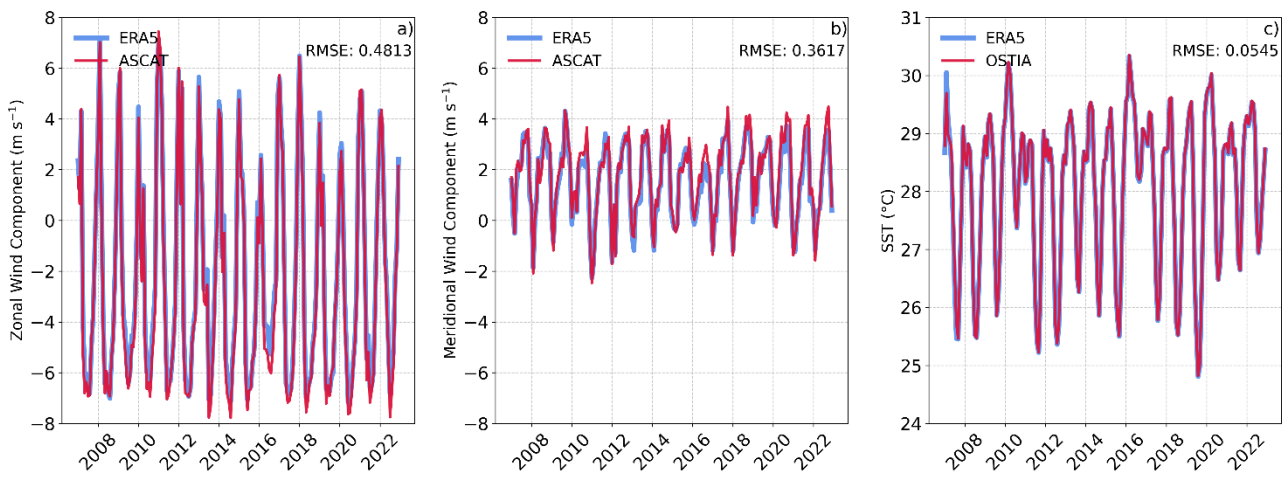


Figure 1. The validation of ERA5 with remote sensing data includes comparing the zonal and meridional winds of ERA5 with ASCAT data, depicted in panels (a) and (b). Panel (c) shows the comparison of ERA5 SST with OSTIA data. The validation process involves calculating the spatial mean within the gray box area illustrated in Figure 2b.

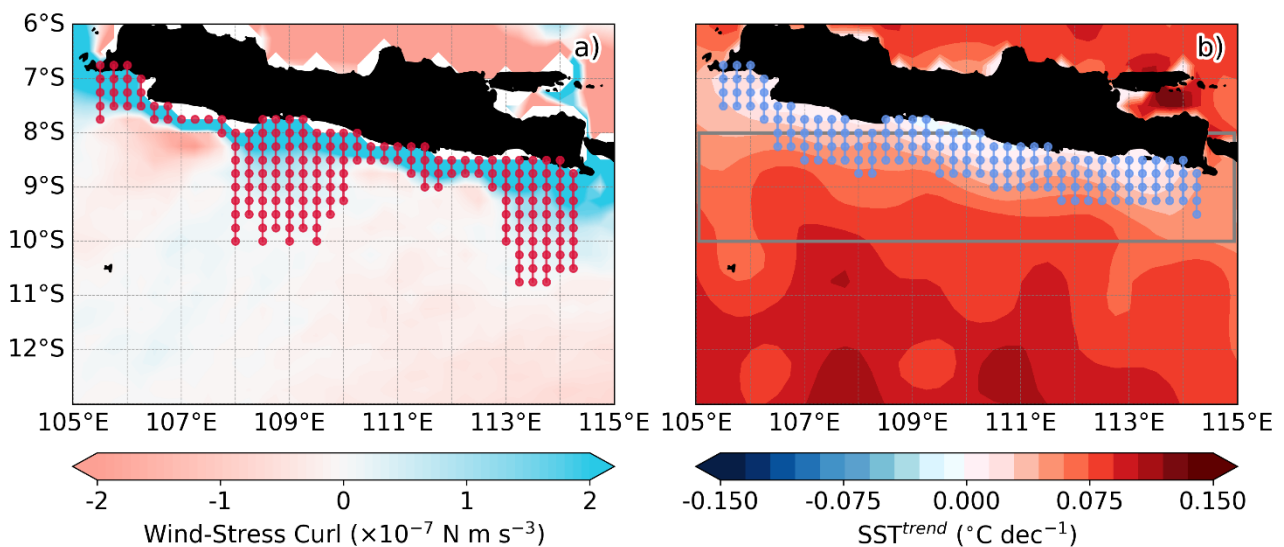


Figure 2. Panel (a) displays the averaged wind-stress curl from July to September, while panel (b) illustrates the SST trend from 1940 to 2023. Red dotted lines indicate positive wind-stress curl values extending from nearshore grid points to the offshore direction. Blue dotted lines delineate the coastal extent where upwelling may influence SST, measured from nearshore grid points to the offshore direction. Gray box in Figure 2b denotes the averaging area for ERA5 data validation as shown in Figure 1.

values were multiplied by -1, ensuring that positive trend values indicate an intensification of wind-driven upwelling, consistent with the other variables.

Comparing Ekman transport and pumping trends is crucial due to their distinct roles in upwelling mechanisms. Methodologies outlined by Pickett and Paduan (2003) and Wang *et al.* (2013) were applied to standardize both Ekman transport and pumping to units of $\text{m}^3 \text{s}^{-1}$ per meter coastline. Ekman pumping was integrated over areas characterized by positive wind-stress curl in the offshore direction at each zonal grid point, as depicted by red dotted lines in Figure 2(a). Unlike Pickett and Paduan (2003), who focused solely on the nearest shore grid point for Ekman transport, the analysis was expanded to include nearby Ekman transport within the coastal area, acknowledging its potential significance in influencing coastal upwelling strength. Ekman transport values were averaged along the offshore direction at each zonal grid point, illustrated by blue dotted lines in Figure 2(b). This methodological approach was also applied to analyze trends in coastal SST. Additionally, total transport, representing the aggregate of Ekman pumping and transport along the coast, was computed, and linear trends were subsequently determined.

After determining the trends for SST and coastal upwelling, both ENSO and IOD indices were processed using the same method. The indices were converted into annual data, representing average values throughout the upwelling period. These were then utilized to compute the trend, revealing the ENSO and IOD pattern.

Result and Discussion

Trends in SST and coastal upwelling

The easiest way to understand the influence of coastal upwelling on the warming rate of SST is by comparing the trend during the upwelling (July to September) and non-upwelling (December to February) periods. Figure 3 illustrates the trends of SST and alongshore winds. In Figure 3a, a positive or warming SST trend is observed along the southern coast of Java. The absence of upwelling during this period causes the SST to warm without hindrance. In contrast, Figure 3c shows a different scenario: along the coast, there is a negative or cooling trend, while the oceanic area experiences a warming trend. This disparity between coastal and oceanic trends during the upwelling period highlights the significant role of coastal upwelling, acting as a natural mechanism countering the SST warming associated with global warming.

Many studies have highlighted the differences in warming rates of SST between oceanic and coastal upwelling areas. Varela *et al.* (2018b) noted that 92% of coastal upwelling areas worldwide have a lower warming rate than adjacent ocean locations, suggesting that upwelling could be a key factor in buffering coastal SST warming. This pattern is consistent with more detailed studies on specific upwelling systems, such as the Canary (Santos *et al.*, 2012a; Sousa *et al.*, 2017), La Guajira (Santos *et al.*, 2016), Somali (DeCastro *et al.*, 2016), and Benguela regions (Santos *et al.*, 2012b), where SST warming trends are lower in coastal upwelling areas compared to adjacent oceanic regions. While it acts as a buffer, upwelling itself is also changing, with a tendency to intensify under global warming conditions. The intensification of upwelling was initially hypothesized by Bakun (1990), who proposed that enhanced alongshore winds could result from the different heating rates between ocean and land due to global warming. This enhancement would contribute to strengthening offshore Ekman transport, a key indicator of coastal upwelling. The hypothesis would work effectively in regions surrounded by large oceans and continents, where a greater land-ocean air pressure gradient could develop. As a result, much research has focused on large-scale, permanent upwelling systems, such as the Eastern Boundary Upwelling Systems (EBUS), as summarized by Satar *et al.* (2023). However, the present results from a smaller, seasonal upwelling area on the southern coast of Java show a cooling trend in SST, which indicates intensifying upwelling. This finding is fascinating because the study area is not directly surrounded by a large continent but is located around an island in the Indonesian archipelago area, which might not support the mechanism of enhanced coastal upwelling as previously hypothesized to answer the cooling trend in SST.

As coastal SST cools, a strengthening of alongshore winds would typically be expected, which would intensify the upwelling through the mechanism of Ekman transport. However, the results in Figure 3d suggest the opposite. A weakening trend in the easterly winds over the coastal area and a strengthening trend farther oceanward were observed. Rather than the typical influence of easterly winds on SST reported in monthly and seasonal analyses (Wirasatriya *et al.*, 2020), the present findings—focusing on yearly differences during the upwelling period only—suggest the contrary. In Figure 3, the spatial distribution of the weakening trend in easterly winds matches the cooling trend in SST, indicating that the cooling SST reduces wind strength. Kim *et al.* (2014) noted that in the upwelling region of East Japan, upwelled cold water reduces wind speed due to air-sea temperature differences, thereby altering atmospheric stability. The more stabilized

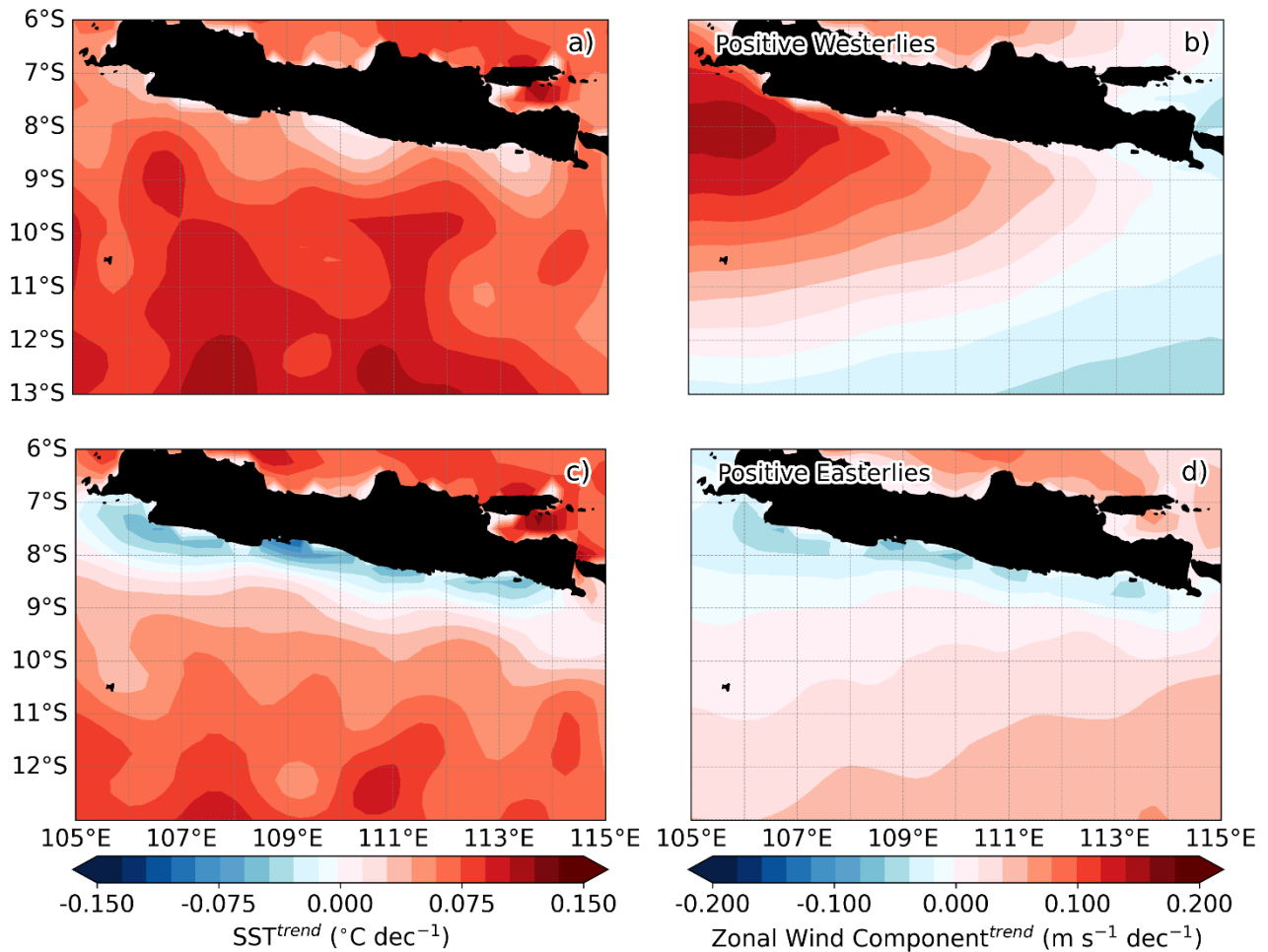


Figure 3. Spatial trends in SST and zonal wind components from 1940 to 2023. Panels (a) and (b) represent the non-upwelling period, averaged over December to February, while panels (c) and (d) depict the peak upwelling period, averaged over July to September. Positive (negative) values indicate an increase (decrease) in trends. In panel (d), the zonal wind component has been multiplied by -1 to clarify the trend, resulting in positive easterly winds.

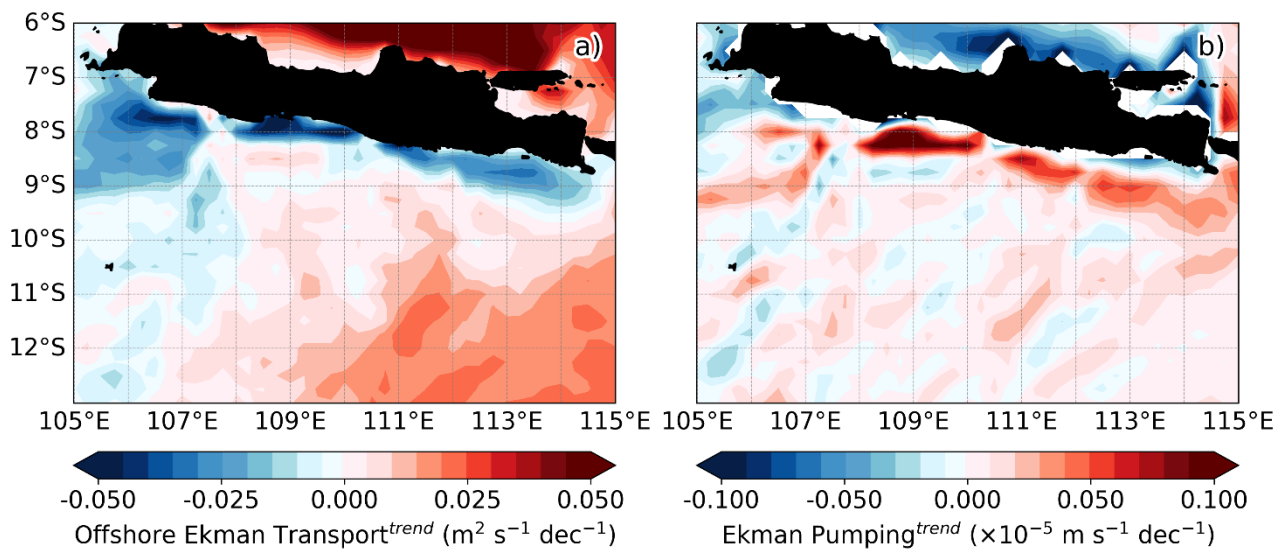


Figure 4. Spatial trends of (a) offshore Ekman transport and (b) Ekman pumping during the upwelling period (averaged over July to September) from 1940 to 2023. Positive values indicate a strengthening of Ekman dynamics, while negative values indicate a weakening

marine atmospheric boundary layer causes less transfer of high-altitude wind speeds to the surface, reducing wind magnitude (Park *et al.*, 2006). This finding suggests a feedback loop of air-sea interaction within the upwelling area. As alongshore winds generate offshore Ekman transport, cold water is brought to the surface. The cold SST stabilizes the marine atmospheric boundary layer, which, in turn, affects the alongshore wind. Because the winds over the ocean are not similarly affected, a gradient in wind strength and Ekman transport is created, increasing the magnitude oceanward. This gradient could potentially enhance positive wind-stress curl, resulting in greater vertical transport of upwelling through Ekman pumping within the coastal region. The results in Figure 4, which show a weakening trend in Ekman transport in the coastal region while the Ekman pumping trend is strengthening, confirm this occurrence. Along the southern coast of Java, this mechanism occurs during the southeast monsoon, when easterly winds generate upwelling. Notably, during the northwest monsoon, when westerly winds prevail, this process might be less likely to occur due to the absence of upwelling-induced SST cooling, which is essential for the feedback mechanism.

In Figure 3b, westerly winds tend to strengthen in the western part and decrease in the eastern part of southern Java. This result does not match the spatial distribution of the SST trend shown in Figure 3a, indicating that westerly winds do not significantly influence SST. During the non-upwelling period, alongshore wind blows from west to east, resulting in Ekman transport toward the shore as it is located in the southern hemisphere. Therefore, it does not influence the SST since there is no deep cold water transported to the surface. A more detailed discussion of the seasonal Ekman dynamics along the southern coast of Java is provided by Wirasatriya *et al.* (2020).

An analysis was conducted to understand why SST continues to show a cooling trend (Figure 3c) in the coastal area despite the weakening trend of easterly winds over time (Figure 3d). Since easterly winds typically drive upwelling through Ekman transport, this inverse relationship suggests that other mechanisms may be sustaining the cooling trend of SST. To investigate these further, long-term trends in both Ekman transport (Figure 4a) and Ekman pumping (Figure 4b) were analyzed, as these processes contribute to upwelling through distinct physical mechanisms. A detailed discussion of these upwelling mechanisms is provided in Pickett and Paduan (2003) and Wang *et al.* (2013). The results indicate that the trend in Ekman transport mirrors the weakening of easterly winds, decreasing near the coast while strengthening offshore. This weakening suggests that upwelling via Ekman transport is

unlikely to be the primary driver of SST cooling in the coastal region. In contrast, upwelling trend via Ekman pumping exhibits a significant increase over the southern coast of Java, with the strongest intensification observed near the coastal region, suggesting that Ekman pumping may have become the dominant driver of SST cooling during the upwelling period. The trend pattern of both Ekman transport and pumping supports the occurrence of an air-sea interaction feedback loop within the upwelling area, as previously explained. However, these observations also suggest a competitive interaction between upwelling trends through Ekman transport and pumping along the coast.

To clarify this issue, the trends of Ekman transport and Ekman pumping were standardized into the same unit for a direct comparison, as shown in Figure 5. The results reveal that changes in Ekman pumping along the coast are significantly greater than those in Ekman transport. This indicates a dominant intensification of upwelling, as represented by the total transport shown in the figure. However, the upwelling trend along the coast does not perfectly match the coastal SST trend distribution. Particularly in the western part of 108°E, where upwelling tends to decrease, yet SST shows a cooling trend. Varela *et al.* (2016) have noted there is a vein of subsurface water that has cooled at a rate higher than 0.3 °C dec⁻¹, is observed to enter from the northwestern part of southern Java, which likely answers to the cooling SST on the western part. But that answer needs to be confirmed in deeper study. Therefore, the unalignment between the spatial trend distribution of upwelling and SST in this study still needs to be further investigated.

The cooling or less warming trend within upwelling areas can result from different causes, depending on the region. DeCastro *et al.* (2016) who used upwelling indicators both from Ekman transport and pumping in Somali, indicate the strengthening of Ekman transport reduces the warming trend of SST, and the Ekman pumping was reported to have less influence. Then, Seo *et al.* (2012) in the U.S. West Coast reported both Ekman transport and pumping predominantly influenced the trend of SST, but within separate areas. However, in this study, the trend of upwelling is better matched to the cooling trend of coastal SST by combining both Ekman transport and pumping, following the agreement on Wirasatriya *et al.* (2020).

Besides the influence of wind-driven upwelling on the SST trend, other research also indicates a local oceanographic phenomenon contributing to the less warming trend in coastal SST. Santos *et al.* (2016) noted the mismatched spatial distribution of the strengthening Ekman transport and cooling SST due

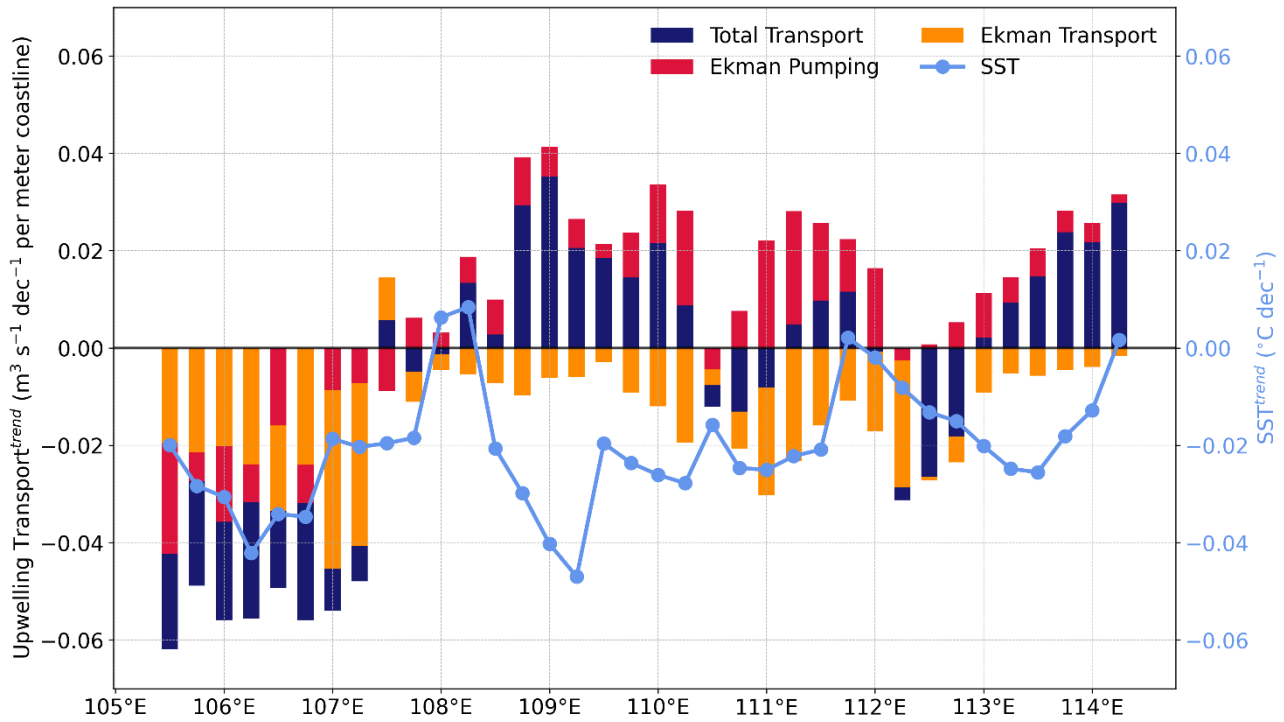


Figure 5. Comparison of coastal trends between wind-driven upwelling by Ekman transport and pumping and their impact on coastal SST trends during the upwelling period (averaged over July to September) from 1940 to 2023. Total transport represents the combined trend of Ekman transport and pumping. The values of Ekman pumping (Ekman transport and SST) are derived from the blue (red) dots in Figure 2a (Figure 2b).

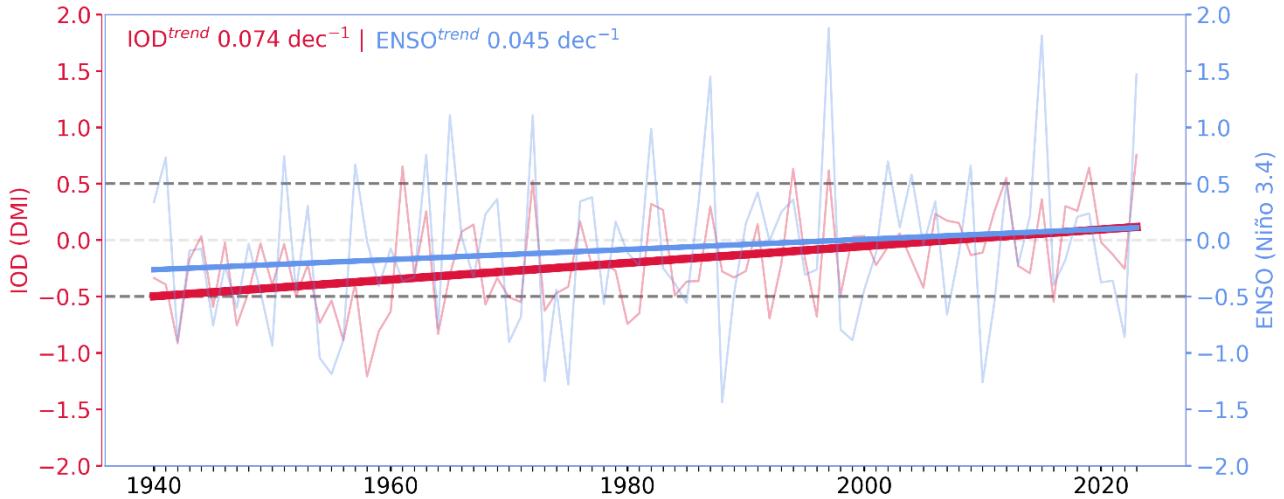


Figure 6. Trends of IOD and ENSO during the upwelling period (averaged over July to September) from 1940 to 2023.

to the local current in la Guajira. Then, Varela *et al.* (2018a) reported coastal cooling in the Yucatan upwelling system, which did not align with the upwelling trend; they hypothesized that local currents were the cause. In this study area, there is a South Java Current that has seasonal characteristics. Generally, this current flows eastward during the northwest monsoon (December to February) and during the first (March to May) and second

(September to November) transitional monsoons this eastward current are being strengthened by the semiannual coastal Kelvin waves from the equatorial Indian Ocean, while during the southeast monsoon (June to August) the direction reverses westward (Ningsih *et al.*, 2021). This is consistent with the report by Wijaya *et al.* (2023), which states that during the northwest and southeast monsoons, the South Java zonal current has weaker coastal

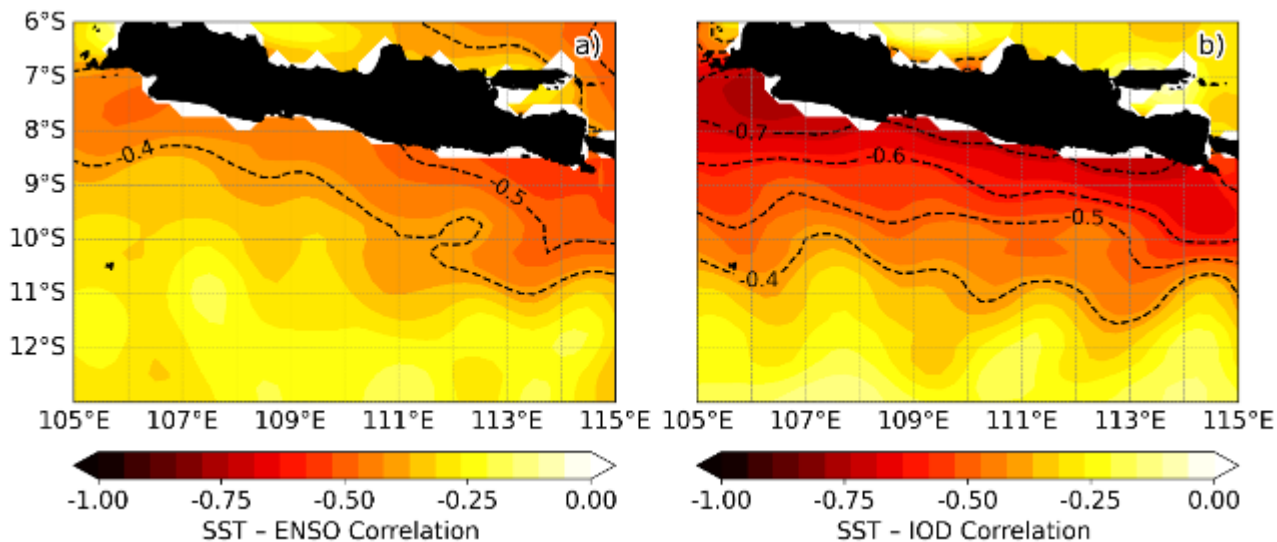


Figure 7. Spatial correlation between SST and the Niño 3.4 index (ENSO) as shown in panel (a), and SST and the DMI (IOD) in panel (b) during the upwelling period (averaged over July to September) from 1940 to 2023.

movement than during the transitional monsoons, even though the current remains strong during the northwest monsoon. The coastal cooling trend of SST is observed during the peak of upwelling period, from July to September, spanning the middle to late southeast monsoon and the start of the second transitional monsoon. However, spatial analysis of the SST trend (Figure 3c) does not show the cooling trend extending either eastward or westward. Instead, it remains mainly concentrated near the coastal area of South Java. Therefore, it is unlikely that the South Java Current has a significant influence on the distribution of the cooling trend of SST in this area, as the current might be at its weak velocities during this period.

In the uncertainty of the causes of coastal cooling along the upwelling system, some research also shows different mechanisms for strengthening upwelling than those proposed by Bakun (1990). For example, García-Reyes *et al.* (2015) showed that in EBUS, the strengthening upwelling is driven by changes in the position of oceanic high-pressure systems, which intensify in a poleward direction. Wang *et al.* (2015) supported this by noting more intense upwelling at higher latitudes but not at lower latitudes. Rykaczewski *et al.* (2015) also revealed consistent latitudinal upwelling zones intensifying near the poles rather than near the equator, due to the poleward migration of atmospheric high-pressure cells. However, the weakening of wind-driven offshore transport, which matches the coastal cooling trend pattern of SST in southern Java, does not seem to align with the causes of weakened winds near the coast due to atmospheric pressure shifts or the mechanisms proposed by Bakun (1990). The results in Figures 3c and 3d suggest that the SST trend

significantly influences the surface wind trend that passes the coastal area during the upwelling period.

Thus far, based on Figures 3a and 3c, the influence of upwelling on the coastal SST cooling trend is clearly evident. In addition, a dominant strengthening of wind-driven coastal upwelling is observed (Figure 5), which fairly aligns with the trend in coastal SST. However, the question remains whether wind trends are the only factor enhancing upwelling or if other mechanisms might also contribute to upwelling intensification along the southern coast of Java.

The influence of ENSO and IOD trends on coastal upwelling

Previous research has highlighted the impact of IOD and ENSO on the southern Java upwelling. It is generally observed that IOD tends to have a more pronounced effect compared to ENSO due to the geographic position closer to the Indian Ocean (Iskandar *et al.*, 2009; Lumban-Gaol *et al.*, 2015; Chen and Han, 2016; Wirasatriya *et al.*, 2020; Lumban-Gaol *et al.*, 2021; Xu *et al.*, 2021; Wen *et al.*, 2023). Both phenomena have two phases: one enhances and the other reduces upwelling along the southern coast of Java. The phases that strengthen upwelling are positive IOD and *El Niño*. During these phases, the thermocline in southern Java generally becomes shallower (Susanto *et al.*, 2001; Horii *et al.*, 2018), facilitating the upward transport of cold deep water to the surface through the wind-driven upwelling system. Therefore, the upwelling during these events results in lower SST compared to the normal upwelling condition.

Positive index values indicate positive IOD and *El Niño* phases. Thus, a positive trend leads to these phases, while a negative trend results in the opposite. Figure 6 illustrates the trend results for IOD and ENSO during the upwelling period. Interestingly, a positive trend is observed for both IOD and ENSO, with a more pronounced change in IOD (0.074 dec^{-1}) than ENSO (0.045 dec^{-1}). The occurrence of more (less) phases of positive (negative) IOD and *El Niño* (*La Niña*) aligns with previous research findings. For further details on ENSO trends, see Yin *et al.* (2009) and Cai *et al.* (2015), and for the IOD, see Ihara *et al.* (2008) and Cai *et al.* (2009).

IOD and ENSO are considered remote influences on upwelling off the southern coast of Java. To verify their effects, the correlation between the IOD and ENSO indices and an upwelling indicator was analyzed. In this case, SST was used as a proxy for upwelling intensity because this phenomenon significantly impacts the thermocline, affecting the transport of cold deep water to the surface by the upwelling process. The results are shown in Figures 7a and b. Both ENSO and IOD exhibit negative correlations, indicating that higher indices correspond to lower SST off the southern coast of Java. The most intriguing aspect is the spatial distribution, where the influence intensifies closer to the coast. This variation clearly demonstrates the roles of ENSO and IOD in enhancing coastal upwelling in this region. Notably, the spatial distribution of these correlations aligns well with SST trend distributions in Figure 3c, further emphasizing this relationship. The strong correlation, particularly from IOD with values exceeding -0.7 near the coast, highlights a significant impact on SST changes over time during the upwelling period. These high correlation values and the corresponding spatial distribution patterns suggest that the coastal cooling trend observed during upwelling periods is primarily driven by IOD and ENSO trends, with Ekman transport and pumping resulting in upwelling acting as a medium being reinforced. Nevertheless, the roles of Ekman transport and pumping remain crucial because, without upwelling, even a strong positive trend from ENSO and IOD would not significantly impact SST. Overall, the combination of ENSO and IOD trends, along with Ekman transport and pumping during the upwelling period, is vital in driving cooling trends in SST along the coast. This highlights the complex interplay between oceanic processes that contribute to changes in SST near the coast.

Based on historical trend research and future projections by Sousa *et al.* (2020), it was found that there is a competition between the influence of SST and wind strength trends. Historically, the trend of wind strength has been more dominant in strengthening coastal upwelling, as hypothesized by

Bakun (1990). However, under extreme global warming scenarios, the SST trend will become more dominant in weakening coastal upwelling by increasing the stratification of the seawater column, which inhibits the vertical movement of currents to the surface. Fortunately, in the southern Java region located in the Indian Ocean, the DMI trend shows a tendency towards a positive IOD and ENSO to *El Niño*. This will allow the SST trend in the coastal upwelling area in southern Java to be maintained or even reduced through the trend of interannual phenomena such as IOD and ENSO.

Conclusion

Analysis of wind-driven upwelling and SST data from 1940 to 2023 along the southern coast of Java, combined with ENSO and IOD indices, yields several important conclusions. First, a warming trend in SST was observed across the entire region during the non-upwelling period, while during the upwelling period, a distinct cooling trend emerged along the coast, underscoring the role of upwelling in mitigating the SST warming trend. The observed cooling SST also contributes to a weakening of the winds over the area by stabilizing the marine atmospheric boundary layer. Second, the results indicate a competitive dynamic in wind-driven upwelling, with the strengthening of Ekman pumping surpassing the weakening of Ekman transport, leading to an overall intensification of wind-driven upwelling. Finally, the positive trends in ENSO and IOD indices during the upwelling period have significantly enhanced the upward movement of cold deep water to the surface, identified as the main factor behind the observed cooling trend in coastal SST. This study highlights the critical role of wind-driven coastal upwelling as a key process, further intensified by positive trends in ENSO and IOD. Continued investigation into future projections in SST and upwelling trends is essential for a more comprehensive understanding and accurate predictions of the implications of coastal upwelling for the fisheries industry.

Acknowledgement

We thank to the European Centre for Medium-Range Weather Forecasts (ECMWF) for providing access to the ERA5 dataset, the European Organization for the Exploitation of Meteorological Satellites (EUMETSAT) for ASCAT data, the UK Met Office for the OSTIA dataset, and the National Oceanic and Atmospheric Administration (NOAA) for the Dipole Mode Index (DMI) and *Niño* 3.4 index. The successful completion of this study was made possible through the use of these valuable datasets, which are publicly accessible as follows: ERA5 is available via <https://doi.org/10.24381/cds.f17050d7>, ASCAT data can be accessed at <https://doi.org/10.48670/>

moi-00183, OSTIA is available at <https://doi.org/10.48670/moi-00165>, and the DMI and Niño 3.4 indices are accessible through NOAA at https://psl.noaa.gov/gcos_wgsp/Timeseries/.

Please note that access to some datasets may require registration or permissions from the respective organizations. We also extend our gratitude to our fellow researchers for their collaboration, which contributed significantly to the success of this study.

References

- Bakun, A. 1990. Global Climate Change and Intensification of Coastal Upwelling. *Sci.*, 247: 198–201. <https://doi.org/10.1126/science.247.4939.198>
- Bunge, L., & Clarke, A. J. 2009. A Verified Estimation of the *El Niño* Index *Niño-3.4* Since 1877. *J. Clim.*, 22(14): 3979–3992. <https://doi.org/10.1175/2009JCLI2724.1>
- Cai, W., Cowan, T., & Sullivan, A. 2009. Recent Unprecedented Skewness Towards Positive Indian Ocean Dipole Occurrences and Its Impact on Australian Rainfall. *Geophys. Res. Lett.*, 36(11): L11705. <https://doi.org/10.1029/2009GL037604>
- Cai, W., Santoso, A., Wang, G., Yeh, S.W., An, S. II, Cobb, K.M., Collins, M., Guilyardi, E., Jin, F.F., Kug, J.S., Lengaigne, M., McPhaden, M.J., Takahashi, K., Timmermann, A., Vecchi, G., Watanabe, M., & Wu, L. 2015. ENSO and Greenhouse Warming. *Nat. Clim. Chang.*, 5(9): 849–859. <https://doi.org/10.1038/nclimate2743>
- Chen, G., & Han, W. 2016. Interannual Variability of Equatorial Eastern Indian Ocean Upwelling: Local versus Remote Forcing. *J. Phys. Oceanogr.*, 46(3): 789–807. <https://doi.org/10.1175/JPO-D-15-0117.s1>
- DeCastro, M., Sousa, M.C., Santos, F., Dias, J.M., & Gómez-Gesteira, M. 2016. How Will Somali Coastal Upwelling Evolve Under Future Warming Scenarios? *Sci. Rep.*, 6: p.30137. <https://doi.org/10.1038/srep30137>
- Donlon, C.J., Martin, M., Stark, J., Roberts-Jones, J., Fiedler, E., & Wimmer, W. 2012. The Operational Sea Surface Temperature and Sea Ice Analysis (OSTIA) System. *Remote Sens. Environ.*, 116: 140–158. <https://doi.org/10.1016/j.rse.2010.10.017>
- García-Reyes, M., Sydeman, W.J., Schoeman, D.S., Rykaczewski, R.R., Black, B.A., Smit, A.J., & Bograd, S.J. 2015. Under Pressure: Climate Change, Upwelling, and Eastern Boundary Upwelling Ecosystems. *Front. Mar. Sci.*, 2: p.109. <https://doi.org/10.3389/fmars.2015.00109>
- Horii, T., Ueki, I., & Ando, K. 2018. Coastal Upwelling Events Along the Southern Coast of Java During the 2008 Positive Indian Ocean Dipole. *J. Oceanogr.*, 74(5): 499–508. <https://doi.org/10.1007/s10872-018-0475-z>
- Ihara, C., Kushnir, Y., & Cane, M.A. 2008. Warming Trend of the Indian Ocean SST and Indian Ocean Dipole from 1880 to 2004. *J. Clim.*, 21(10): 2035–2046. <https://doi.org/10.1175/2007JCLI1945.1>
- Iskandar, I., Rao, S.A., & Tozuka, T. 2009. Chlorophyll-a Bloom Along the Southern Coasts of Java and Sumatra During 2006. *Int. J. Remote Sens.*, 30(3): 663–671. <https://doi.org/10.1080/01431160802372309>
- Kim, T. S., Park, K. A., Li, X., & Hong, S. 2014. SAR-derived Wind Fields at the Coastal Region in the East/Japan Sea and Relation to Coastal Upwelling. *Int. J. Remote Sens.*, 35(11–12): 3947–3965. <https://doi.org/10.1080/0143116.2014.916438>
- Koropitan, A.F., Kholilullah, I., & Yusfiandayani, R. 2021. Modeling Mackerel Tuna (*Euthynnus affinis*) Habitat in Southern Coast of Java: Influence of Seasonal Upwelling and Negative IOD. *Hayati: J. Biosci.*, 28(4): 271–285. <https://doi.org/10.4308/HJB.28.4.271-285>
- Lumban-Gaol, J., Leben, R.R., Vignudelli, S., Mahapatra, K., Okada, Y., Nababan, B., Mei-Ling, M., Amri, K., Arhatin, R. E., & Syahdan, M. 2015. Variability of Satellite-derived Sea Surface Height Anomaly, and Its Relationship with Bigeye Tuna (*Thunnus obesus*) Catch in the Eastern Indian Ocean. *Eur. J. Remote Sens.*, 48: 465–477. <https://doi.org/10.5721/EuJRS20154826>
- Lumban-Gaol, J., Siswanto, E., Mahapatra, K., Natih, N.M.N., Nurjaya, I. W., Hartanto, M.T., Maulana, E., Adrianto, L., Rachman, H.A., Osawa, T., Rahman, B.M.K., & Permana, A. 2021. Impact of the Strong Downwelling (Upwelling) on Small Pelagic Fish Production During the 2016 (2019) Negative (Positive) Indian Ocean Dipole Events in the Eastern Indian Ocean off Java. *Climate*, 9(2): 1–11. <https://doi.org/10.3390/cli9020029>
- Mercado, J.M., Cortés, D., Ramírez, T., & Gómez, F. 2012. Decadal Weakening of the Wind-Induced

- Upwelling Reduces the Impact of Nutrient Pollution in the Bay of Málaga (Western Mediterranean Sea). *Hydrobiología*, 680(1): 91–107. <https://doi.org/10.1007/s10750-011-0906-y>
- Ningsih, N.S., Sakina, S.L., Susanto, R.D., & Hanifah, F. 2021. Simulated Zonal Current Characteristics in the Southeastern Tropical Indian Ocean (SETIO). *Ocean Sci.*, 17(4): 1115–1140. <https://doi.org/10.5194/os-17-1115-2021>
- Park, K.A., Cornillon, P., & Codiga, D.L. 2006. Modification of Surface Winds Near Ocean Fronts: Effects of Gulf Stream Rings on Scatterometer (QuikSCAT, NSCAT) Wind Observations. *J. Geophys. Res: Oceans*, 111(3): C03021. <https://doi.org/10.1029/2005JC003016>
- Pickett, M.H., & Paduan, J.D. 2003. Ekman Transport and Pumping in the California Current Based on the U.S. Navy's High-resolution Atmospheric Model (COAMPS). *J. Geophys. Res.: Oceans*, 108(10): C10. <https://doi.org/10.1029/2003jc001902>
- Rachman, H.A., Gaol, J.L., Syamsudin, F., & As-Syakur, A. 2020. Influence of Coastal Upwelling on Sea Surface Temperature Trends Banda Sea. *IOP Conf. Ser.:Earth Environ. Sci.*, 429(1): p.012015. <https://doi.org/10.1088/1755-1315/429/1/012015>
- Remmers, T., Cawkwell, F., Desmond, C., Murphy, J., & Politi, E. 2019. The Potential of Advanced Scatterometer (ASCAT) 12.5 km Coastal Observations for Offshore Wind Farm Site Selection in Irish Waters. *Energies*, 12(2): p206. <https://doi.org/10.3390/en12020206>
- Rykaczewski, R.R., Dunne, J.P., Sydeman, W.J., García-Reyes, M., Black, B.A., & Bograd, S.J. 2015. Poleward Displacement of Coastal Upwelling-favorable Winds in the Ocean's Eastern Boundary Currents Through the 21st Century. *Geophys. Res. Lett.*, 42(15): 6424–6431. <https://doi.org/10.1002/2015GL064694>
- Saji, N., Goswami, B., Vinayachandran, P.N., & Yamagata, T. 1999. A Dipole Mode in the Tropical Indian Ocean. *Nature*, 401: 360–363. <https://doi.org/https://doi.org/10.1038/43854>
- Santos, F., DeCastro, M., Gómez-Gesteira, M., & Álvarez, I. 2012a. Differences in Coastal and Oceanic SST Warming Rates Along the Canary Upwelling Ecosystem from 1982 to 2010. *Cont. Shelf Res.*, 47: 1–6. <https://doi.org/10.1016/j.csr.2012.07.023>
- Santos, F., Gomez-Gesteira, M., deCastro, M., & Alvarez, I. 2012b. Differences in Coastal and Oceanic SST Trends due to the Strengthening of Coastal Upwelling Along the Benguela Current System. *Cont. Shelf Res.*, 34: 79–86. <https://doi.org/10.1016/j.csr.2011.12.004>
- Santos, F., Gómez-Gesteira, M., Varela, R., Ruiz-Ochoa, M., & Días, J. M. 2016. Influence of Upwelling on SST Trends in la Guajira System. *J. Geophys. Res. Oceans*, 121(4): 2469–2480. <https://doi.org/10.1002/2015JC011420>
- Satar, M.N., Akhir, M.F., Zainol, Z., & Chung, J.X. 2023. Upwelling in Marginal Seas and Its Association with Climate Change Scenario—A Comparative Review. *Climate*, 11(7): p.151. <https://doi.org/10.3390/cli11070151>
- Seo, H., Brink, K.H., Dorman, C.E., Koracin, D., & Edwards, C.A. 2012. What Determines the Spatial Pattern in Summer Upwelling Trends on the U.S. West Coast? *J. Geophys. Res.: Oceans*, 117(8): c08012. <https://doi.org/10.1029/2012JC008016>
- Sousa, M.C., Alvarez, I., deCastro, M., Gomez-Gesteira, M., & Dias, J. M. 2017. Seasonality of coastal upwelling trends under future warming scenarios along the southern limit of the canary upwelling system. *Prog. Oceanogr.*, 153: 16–23. <https://doi.org/10.1016/j.pocean.2017.04.002>
- Sousa, M.C., Ribeiro, A., Des, M., Gomez-Gesteira, M., deCastro, M., & Dias, J.M. 2020. NW Iberian Peninsula Coastal Upwelling Future Weakening: Competition Between Wind Intensification and Surface Heating. *Sci. Total Environ.*, 703: p.134808. <https://doi.org/10.1016/j.scitotenv.2019.134808>
- Stewart, R.H. 2008. Introduction to Physical Oceanography. Texas A & M University. 331 pp.
- Susanto, R.D., Gordon, A.L., & Zheng, Q. 2001. Upwelling Along the Coasts of Java and Sumatra and Its Relation to ENSO. *Geophys. Res. Lett.*, 28(8): 1599–1602. <https://doi.org/10.1029/2000GL011844>
- Varela, R., Álvarez, I., Santos, F., DeCastro, M., & Gómez-Gesteira, M. 2015. Has Upwelling Strengthened Along Worldwide Coasts Over 1982-2010? *Sci. Rep.*, 5: p.10016. <https://doi.org/10.1038/srep10016>

- Varela, R., Costoya, X., Enriquez, C., Santos, F., & Gómez-Gesteira, M. 2018a. Differences in Coastal and Oceanic SST Trends North of Yucatan Peninsula. *J. Mar. Syst.*, 182: 46–55. <https://doi.org/10.1016/j.jmarsys.2018.03.006>
- Varela, R., Lima, F.P., Seabra, R., Meneghesso, C., & Gómez-Gesteira, M. 2018b. Coastal Warming and Wind-driven Upwelling: A Global Analysis. *Sci. Total Environ.*, 639: 1501–1511. <https://doi.org/10.1016/j.scitotenv.2018.05.273>
- Varela, R., Santos, F., Gómez-Gesteira, M., Álvarez, I., Costoya, X., & Días, J.M. 2016. Influence of Coastal Upwelling on SST Trends Along the South Coast of Java. *PLoS One*, 11(9): p.e0162122. <https://doi.org/10.1371/journal.pone.0162122>
- Wamdi, G. 1988. The WAM Model—A Third Generation Ocean Wave Prediction Model. *J. Phys. Oceanogr.*, 18: 1775–1810. [https://doi.org/10.1175/1520-0485\(1988\)018<1775:TWMTGO>2.0.CO;2](https://doi.org/10.1175/1520-0485(1988)018<1775:TWMTGO>2.0.CO;2)
- Wang, D., Gouhier, T.C., Menge, B.A., & Ganguly, A.R. 2015. Intensification and Spatial Homogenization of Coastal Upwelling Under Climate Change. *Nature*, 518(7539): 390–394. <https://doi.org/10.1038/nature14235>
- Wang, D., Wang, H., Li, M., Liu, G., & Wu, X. 2013. Role of Ekman Transport Versus Ekman Pumping in Driving Summer Upwelling in the South China Sea. *J. Ocean Univ. China*, 12(3): 355–365. <https://doi.org/10.1007/s11802-013-1904-7>
- Wen, C., Wang, Z., Wang, J., Li, H., Shi, X., Gao, W., & Huang, H. 2023. Variation of the Coastal Upwelling off South Java and Their Impact on Local Fishery Resources. *J. Oceanol. Limnol.*, 41(4): 1389–1404. <https://doi.org/10.1007/s00343-022-2031-3>
- Wijaya, Y.J., Wisha, U.J., Rejeki, H.A., & Ismunarti, D. H. 2023. Variability of the South Java Current From 1993 to 2021, and Its Relationship to ENSO and IOD Events. *Asia Pac. J. Atmos. Sci.*, <https://doi.org/10.1007/s13143-023-00336-2>
- Wirasatriya, A., Setiawan, J.D., Sugianto, D.N., Rosyadi, I. A., Haryadi, H., Winarso, G., Setiawan, R. Y., & Susanto, R. D. 2020. Ekman Dynamics Variability Along the Southern Coast of Java Revealed by Satellite Data. *Int. J. Remote Sens.*, 41(21): 8475–8496. <https://doi.org/10.1080/01431161.2020.1797215>
- Wirasatriya, A., Susanto, R. D., Kunarso, K., Jalil, A. R., Ramdani, F., & Puryajati, A. D. 2021. Northwest Monsoon Upwelling within the Indonesian Seas. *Int. J. Remote Sens.*, 42(14): 5437–5458. <https://doi.org/10.1080/01431161.2021.1918790>
- Xu, T., Wei, Z., Li, S., Susanto, R.D., Radiarta, N., Yuan, C., Setiawan, A., Kuswardani, A., Agustiadi, T., & Trenggono, M. 2021. Satellite-observed Multi-scale Variability of Sea Surface Chlorophyll-a Concentration Along the South Coast of the Sumatra-Java Islands. *Rem. Sens.*, 13(14): p.2817. <https://doi.org/10.3390/rs13142817>
- Yin, Y., Xu, Y., & Chen, Y. 2009. Relationship Between Flood/Drought Disasters and ENSO From 1857 to 2003 in the Taihu Lake Basin, China. *Quat. Int.*, 208(1–2): 93–101. <https://doi.org/10.1016/j.quaint.2008.12.016>
- Zhang, C. 2021. Responses of Summer Upwelling to Recent Climate Changes in the Taiwan Strait. *Rem. Sens.*, 13(7): p.1386.. <https://doi.org/10.3390/rs13071386>